HYBRID ELECTRICAL STIMULATION TRACKING CONTROL OF THE ANKLE

Q.Wang *
Department of Electrical
and Computer Engineering
University of Florida
Gainesville, Florida 32611
Email: qiangw@ufl.edu

R. Kamalapurkar
R. Downey
W. E. Dixon
Department of Mechanical
and Aerospace Engineering
University of Florida
Gainesville, Florida 32611
Email: {rkamalapurkar, ryan2318, wdixon}@ufl.edu

ABSTRACT

Functional electrical stimulation (FES) is an effective rehabilitation tool for gait retraining for individuals suffering from various neurological disorders. Traditionally, FES is only delivered to activate ankle dorsiflexor muscles during the swing phase of the gait to correct "foot drop". Recent research indicates that improved functional ambulation can be achieved by delivering FES to both the plantarflexor and dorsiflexor muscles during gait. Closed-loop electrical stimulation has the potential to yield positive rehabilitative outcomes by enabling accurate and precise limb motions during gait retraining. Naturally, the motion of ankle during gait is an event-driven system combining continuous evolution of the angle between the foot and shank, alternate moving segments of the foot and shank, and alternate activation of the plantarflexor and dorsiflexor muscles. A switched sliding mode based controller is developed to ensure that the ankle tracks a designed or recorded normal trajectory during gait which can be used for gait retraining. Semi-global asymptotic tracking of the hybrid controller is analyzed using multiple Lyapunov functions and the performance is illustrated through simulations.

1 Introduction

Of the 730,000 individuals who survive a stroke each year, 73% have residual disability [1]. Stroke has significant impact on walking ability resulting in characteristic post stroke gait. For example, inadequate dorsiflexion during swing phase and decreased plantarflexion force generation during the stance phase are both common impairments of post stroke gait causing foot dragging and slapping, larger metabolic cost on walking, slow walking speed, and gait asymmetry. By delivering pulsed electrical current into affected muscles or nerves, desired muscle contractions can be obtained, which is referred to as neuromuscular electrical stimulation (NMES), and when used for performing functional tasks, it is known as functional electrical stimulation (FES). FES is commonly used as an effective rehabilitation tool to enable muscle training and gait correction to improve post stoke recovery and achieve daily life independence. Traditionally with the help of foot switches or employing tilt sensors, FES can be delivered to activate ankle dorsiflexor muscles during the swing phase of the gait to correct "foot drop", a common symptom caused by stroke, spinal cord injury and other neurological diseases. However, stimulating ankle dorsiflexor muscles only during the swing phase does not prevent foot slap, decreased swing phase knee flexion, or slow walking speed. Resent research [2, 3] has shown that delivering FES to both the plantarflexor and dorsiflexor muscles during gait can help to correct post stroke gait deficits at multiple joints (ankle and knee) during both the swing and stance phases of gait resulting in improved functional ambulation. These FES treatments are typically applied open-loop and have led to some promising results including some commercial products. However, such approaches offer limited precision and predictability without feedback, and typically over stimulate the muscle potentially leading to a more rapid onset of fatigue.

Closed-loop NMES has the potential to stimulate muscle and enable the rehabilitative outcome by achieving accu-

*Address all correspondence to this author.
This research is supported in part by the NSF CAREER award CMS-0547448 and NSF award number 0901491.

rate/precise limb motions for gait retraining. Various closed-loop controllers have been developed for NMES such as PID (proportional–integral–derivative) –based controllers (cf. [4–6]), neural networks-based controllers (cf. [7–11]), and robust controllers such as sliding mode control [12] and RISE (robust integral of the sign of the error) -based controllers [13, 14].

The aforementioned controllers are developed (with associate stability analysis) without considering the discrete nature of a walking gait. As described in [15] (see also Section II), the ankle motion is continuous during normal gait, but the actuator alternates between plantarflexor and dorsiflexor muscles and the moving segment is the foot during initial stance phase and swing phase while the moving segment is the shank from toe strike to toe off. The ankle movement is a continuous evolution of the angle between foot and shank, yet an isolated discrete signal is needed to denote the transition between plantarflexion and dorsiflexion. The transition is important to maintain a continuous ankle motion. The switching property of gait control suggests the need to model and analyze the ankle motion control system using hybrid systems control theory. Generally, coexistence and interaction between continuous dynamics and discrete events (such as switching) in a system result in unique properties that are not inherited from individual subsystems. A well known example can be found in [16] that shows switching between globally exponentially stable subsystems does not guarantee the stability of the hybrid dynamic system. The stability of switched systems depends on the interplay of the dynamics of subsystems and the properties of the switching signals. Common Lyapunov functions, converse Lyapunov theorems and multiple Lyapunov functions are commonly used tools for the stability analysis of hybrid dynamic systems [16, 17].

In this paper, ankle motion control is modeled as a hybrid system and a switched controller comprised of multiple sliding mode based controllers is designed for the first time to enable the ankle to track desired trajectories during gait. Semi-global asymptotic tracking result of the switched controller during gait is analyzed based on multiple Lyapunov functions and the performance is illustrated though simulations.

2 Dynamic Model

The dynamics of a muscle-limb system can be segmented into two subsystems: the muscle activation and contraction dynamics related to muscle force generation, and the body segmental dynamics including passive muscle and joint mechanical properties, inertial effects, and gravity effects of the system. These dynamics can be modeled as [5, 14]

$$M_I + M_e + M_g + M_v + \tau_{ds} = \tau. \tag{1}$$

In (1), $M_I(\ddot{q}) \in \mathbb{R}$ denotes the inertia of the limb about the joint, $M_e(q) \in \mathbb{R}$ denotes the elastic effects due to joint stiffness, $M_g(q) \in \mathbb{R}$ denotes the gravitational component, $M_v(\dot{q}) \in \mathbb{R}$ denotes the viscous effects due to damping in the musculotendon complex, $\tau_{ds}(t) \in R$ is considered as an unknown bounded disturbance which represents an unmodeled reflex activation of the muscle (e.g., muscle spasticity) and other unknown unmodeled phenomena, and $\tau(t) \in \mathbb{R}$ denotes the muscle torque produced at the joint. The angular position, velocity, and acceleration of the limb about the joint is denoted by $q(t)$, $\dot{q}(t)$, $\ddot{q}(t) \in \mathbb{R}$, respectively. The gravitational effects can be modeled as

$$M_g = -mglsin(q), \tag{2}$$

where $m \in R$ denotes the unknown mass of the shank or foot, $l \in R$ is the unknown distance between the ankle and the lumped center of mass of the shank or foot, and $g \in R$ denotes the gravitational acceleration. The elastic effects are modeled based on empirical findings by Ferrarin and Pedotti in [18] as

$$M_e = -k_1(exp(-k_2\left(q+\frac{\pi}{2}\right)))(q+\frac{\pi}{2}-k_3), \tag{3}$$

where $k_1, k_2, k_3 \in R$ are unknown positive coefficients. As shown in [5], the viscous moment can be modeled as

$$M_v = B_1 tanh(-B_2\dot{q}) - B_3\dot{q}, \tag{4}$$

where B_1, B_2, $B_3 \in R$ are unknown positive constants. Further, the inertial component $M_I(\ddot{q}) \in \mathbb{R}$ is defined as

$$M_I = J\ddot{q}, \tag{5}$$

where $J \in \mathbb{R}$ denotes the unknown inertia of the shank or foot. The relationship between generated muscle torque and the applied electrical stimulus, denoted by $u(t) \in \mathbb{R}$, can be developed as

$$\tau = \zeta u, \tag{6}$$

where $\zeta(q,\dot{q}) \in \mathbb{R}$ denotes the combined effect of the positive moment arm and the positive nonlinear muscle contraction mapping function. For complete details of the dynamics development, see [14].

Assumption 1. Based on the results in [14], $\zeta(q,\dot{q})$ is assumed to be a continuously differentiable, positive, and monotonic function that can be upper and lower bounded by some known positive constants.

Assumption 2. The disturbance term $\tau_{ds}(t)$ is assumed to be bounded. This assumption is reasonable for typical disturbances such as muscle spasticity and load changes during functional tasks.

To facilitate the subsequent analysis, the expression in (1) is rewritten as

$$J_{\zeta}\ddot{q} = -M_{\zeta} - \tau_{d\zeta} + u, \tag{7}$$

where $J_{\zeta}(q,\dot{q}), M_{\zeta}(q,\dot{q}), \tau_{d\zeta}(q,\dot{q},t) \in \mathbb{R}$ are defined as

$$J_{\zeta} = J\zeta^{-1},\ M_{\zeta} = (M_e + M_g + M_v)\zeta^{-1},\ \tau_{d\zeta} = \tau_{ds}\zeta^{-1}. \tag{8}$$

Based on Assumptions 1 and 2, the following inequalities can be developed

$$\xi_0 \leq |J_{\zeta}| \leq \xi_1,\ |\tau_{d\zeta}| \leq \xi_2, \tag{9}$$

where $\xi_0, \xi_1, \xi_2 \in \mathbb{R}$ are known positive constants.

While the arcs of ankle motion during walking are not large, they are critical for progression and shock absorption during stance [15]. During normal gait, the arcs of ankle motion continuously plantarflex and then dorsiflex. During the stance phase, the ankle plantarflexes, dorsiflexes and then plantarflexes again. During the swing phase the ankle only dorsiflexes. The activated muscles switch between dorsiflexor and plantarflexor muscles during each gait cycle.

Each gait cycle starts from heel strike, the beginning of the stance phase. The ankle position starts at neutral. The dorsiflexor muscle (tibialis anterior) becomes active immediately after heel strike to toe strike to decelerate the rate of plantar flexion, which contributes to shock absorption, body weight acceptance, and limb progression. Throughout heel strike to toe strike phase, the moving segment is the foot and the leg remains relatively stationary. After toe strike, the forefoot contacts the floor and the foot becomes stationary. The moving segment is the leg (shank). The plantarflexor (calf muscles) gradually increases eccentric contraction to control ankle dorsiflexion and provide critical stabilization that allows both the foot and tibia to move forward and provide forward propulsion (push-off). By the end of terminal stance, with the weight shifting to the other leg, the stabilizing force in the foot goes away, and the foot is free to plantarflex corresponding to the activation of plantarflexor muscle (gastrosoleus) while the onset of dorsiflexor muscle (tibialis anterior) activity decelerates the foot fall (this coactivation of dorsiflexor and plantarflexor muscles is modeled as the activation of plantarflexor muscles only for simplicity). At toe-off, the swing phase begins and the second arc of dorsiflexion starts. Dorsiflexor muscles activate again to lift the foot clear of the ground. At the end of the swing phase the ankle position returns to neutral preparing for heel contact [15]. A summary of the gait cycle is provided in Table1.

To capture the switching property of gait cycle, the ankle dynamics can be modeled as

$$J_{\zeta_{\sigma}}\ddot{q} = -M_{\zeta_{\sigma}} - \tau_{d\zeta_{\sigma}} + u_{\sigma}, \tag{10}$$

where $\sigma : [0,\infty) \to \mathcal{P}$, denotes a piecewise constant switching signal which can be expressed as

$$\sigma = p,\ \ p \in \mathcal{P} \triangleq \{1,\ 2,\ 3,\ 4\}. \tag{11}$$

For example, $\sigma(t)$ could be the signal from foot switches indicating the transition of gait phases.

3 Control Objective

The control objective is to ensure that the ankle follows designed or recorded ankle trajectories during normal gait, which is essential in rehabilitative exercises and function restoration.

To quantify the tracking objective, an angular position tracking error, denoted by $e(t) \in \mathbb{R}$, is defined as

$$e \triangleq q_d - q, \tag{12}$$

where $q_d(t) \in \mathbb{R}$ denotes the desired limb angular position. To facilitate the subsequent control design and stability analysis, a filtered tracking error, denoted by $r(t) \in \mathbb{R}$, is defined as

$$r \triangleq \dot{e} + \alpha e, \tag{13}$$

where $\alpha \in \mathbb{R}$ is a positive constant gain.

4 Controller Design

Controllers are designed for each subsystem individually, which is indicated by a subscript $p \in \mathcal{P} \triangleq \{1,\ 2,\ 3,\ 4\}$. Taking the derivative of (13), multiplying both sides by $J_{\zeta p,}$ and using (10) and (12), yields

$$J_{\zeta p}\dot{r} = J_{\zeta p}(\ddot{q}_d + \alpha\dot{e}) + M_{\zeta_p} + \tau_{d\zeta p} - u_p. \tag{14}$$

Based on (14) and the subsequent stability analysis, the control law is defined as

$$u_p = k_{s_p}r + e + \beta_p sgn(r) + k_c, \tag{15}$$

where $k_{s_p}, \beta_p, k_c \in \mathbb{R}$ are adjustable gains, and $y(t) \in \mathbb{R}^2$ is defined as

$$y = [e\ r]. \tag{16}$$

After substituting (15) into (14) and performing some algebraic manipulation, the closed-loop error dynamics can be expressed as

$$\begin{aligned} J_{\zeta_p}\dot{r} = &-\frac{1}{2}\dot{J}_{\zeta_p}r + \tilde{N}_p + N_{D_p} \\ &-k_{s_p}r - e - \beta_p sgn(r) - k_c, \end{aligned} \tag{17}$$

	Gait Cycle			
	Stance Phase			Swing Phase
Ankle Motion	Planta-	Dorsi-	Planta-	Dorsi-
Activated Muscle Group	Dorsi-	Planta-	Planta-	Dorsi-
Moving Part	Foot	Shank	Shank	Foot
Switching Signal	1	2	3	4

Table 1. Summary of ankle motions, activated muscle groups, and moving parts during gait cycle.

where the auxiliary functions $N_p(\dot{e},r,q,\dot{q},\ddot{q},\ddot{q}_d)$, $N_{D_p}(q_d,\dot{q}_d,\ddot{q}_d,t)$, $\tilde{N}_p(\dot{e},r,q,\dot{q},\ddot{q},q_d,\dot{q}_d,\ddot{q}_d,t)\in\mathbb{R}$ are defined as

$$N_p \triangleq \frac{1}{2}\dot{J}_{\zeta p}r + J_{\zeta p}(\ddot{q}_d+\alpha\dot{e}) + M_{\zeta_p}, \tag{18}$$

$$\tilde{N}_p \triangleq N_p - J_{\zeta p}(q_d,\dot{q}_d)\ddot{q}_d - M_{\zeta_p}(q_d,\dot{q}_d),$$

$$N_{D_p} \triangleq J_{\zeta p}(q_d,\dot{q}_d)\ddot{q}_d + M_{\zeta_p}(q_d,\dot{q}_d) + \tau_{d\zeta p} - k_c.$$

The following inequality can be developed based on Assumption 1 and 2,

$$\left|N_{D_p}\right| \leq \xi_{4_p}, \tag{19}$$

where $\xi_{4_p}\in\mathbb{R}$ is a known positive constant. The control gain k_c can be adjusted to reduce ξ_{4_p}. The Mean Value Theorem can be used to develop the following upper bound

$$\left|\tilde{N}_p\right| \leq \rho_p(\|y\|)\|y\|, \tag{20}$$

where $\rho_p(\|y\|)\in\mathbb{R}$ is a positive, globally invertible function.

5 Stability Analysis

For each gait cycle, let $t_0=0$ and $t_4=T$, where $T\in\mathbb{R}$ denotes the period of a gait cycle. The time interval between two switches, denoted by $T_i\in\mathbb{R}$, $i=1,2,3,4$, is defined as

$$T_i = t_i - t_{i-1}, \tag{21}$$

where t_i denote the switching times. Define $\gamma_{1_p},\gamma_{2_p}\in\mathbb{R}$, $p\in\mathcal{P}$ as

$$\gamma_{1_p} \triangleq \frac{1}{2}\min(1,\xi_{0_p}), \tag{22}$$

$$\gamma_{2_p} \triangleq \frac{1}{2}\max(1,\xi_{1_p}), \tag{23}$$

where ξ_{0_p}, ξ_{1_p} are introduced in (9).

Theorem 1. *The control law $u(t)=u_{\sigma(t)}(t)$ ensures all closed-loop signals are bounded and semi-global asymptotic tracking in the sense that $|e(t)|\to 0$ as $t\to\infty$, provided the sufficient conditions*

$$\beta_p > \xi_{4_p}, \quad p\in\mathcal{P}, \tag{24}$$

$$\sum_{p=1}^{4}\frac{\gamma_{3_p}}{\gamma_{2_p}}T_p > \sum_{p=1}^{4}\log\left(\frac{\gamma_{2_p}}{\gamma_{1_p}}\right), \tag{25}$$

are satisfied, where $\beta_p\in\mathbb{R}$ is introduced in (15), ξ_{4_p} is introduced in (19), $\gamma_{1_p},\gamma_{2_p}\in\mathbb{R}$, are introduced in (22) and (23), and $\gamma_{3_p}\in\mathbb{R}$ are positive constants determined by the initial condition of the system and the control gains α and k_{s_p}.

Proof. For each phase indicated by $\sigma(t)$, consider a continuously differentiable, radially unbounded, positive definite function $V_p(e,r,t)\in\mathbb{R}$, $p\in\mathcal{P}$ defined as

$$V_p = \frac{1}{2}e^2 + \frac{1}{2}r^2 J_{\zeta_p}. \tag{26}$$

Using (9), $V_p(e,r,t)$ can be upper and lower bounded as

$$\gamma_{1_p}\|y\|^2 \leq V_p \leq \gamma_{2_p}\|y\|^2, \tag{27}$$

where $\gamma_{1_p},\gamma_{2_p}\in\mathbb{R}$ are defined in (22) and (23). After taking the time derivative of (26), and using (13) and (17), $\dot{V}_p(e,r,t)$ can be expressed as

$$\dot{V}_p = -\alpha e^2 - k_{s_p}r^2 - \beta_p|r| + \tilde{N}_p r + N_{D_p}r.$$

Using (20) and (19), $\dot{V}_p(t)$ can be upperbounded as

$$\begin{aligned}\dot{V}_p \leq & -\alpha e^2 - k_{s_p}r^2 + \rho_p(\|y\|)|r|\|y\| \\ & -\beta_p|r| + \xi_{5_p}|r|,\end{aligned}$$

which can be further upperbounded as

$$\dot{V}_p \leq -\left(min(\alpha, \frac{3}{4}k_{s_p}) - \frac{\rho_p^2(\|y\|)}{k_{s_p}}\right)\|y\|^2 \leq -\gamma_{3_p}\|y\|^2, \quad (28)$$

provided the sufficient conditions in (24) is satisfied, and where $\gamma_{3p} \in \mathbb{R}$ is a positive constant provided α and k_{s_p} are selected sufficiently large based on the initial condition of the activated subsystem. The region of attraction $\mathcal{D}_p$ is defined as

$$\mathcal{D}_p \triangleq \left\{ y(t) \subset \mathbb{R}^2 \mid \|y\| \leq \rho_p^{-1}\left(\sqrt{min(\alpha, \frac{3}{4}k_{s_p})k_{s_p}}\right)) \right\}, \quad (29)$$

That is, the region of attraction can be made arbitrarily large to include any initial conditions by increasing the control gain α and k_{s_p} (i.e., a semi-global type of stability result). Using (27) and (28), and solving the resulting differential equation yields

$$V_p(t) \leq V_p(0)e^{-\lambda_p t}, \quad (30)$$

where $\lambda_p \in \mathbb{R}$ is a constant defined as

$$\lambda_p \triangleq \frac{\gamma_{3_p}}{\gamma_{2_p}}. \quad (31)$$

Provided the condition in (24) is satisfied, the control input and all the closed-loop signals are bounded during $\sigma(t) = p$ in $\mathcal{D}_p$.

Even though each controller is exponentially stable, additional development is required to examine the stability of the composite system. To this end, (27) can be used to conclude

$$V_{\sigma(t_i)}(t_i) \leq \mu_i V_{\sigma(t_i - 1)}(t_i), \quad (32)$$

where $\sigma(t_i) = i+1$, and the constant $\mu_i \in \mathbb{R}$, $i = 1,2,3,4$ is defined as

$$\mu_i \triangleq \frac{\gamma_{2_{\sigma(t_i)}}}{\gamma_{1_{\sigma(t_{i-1})}}}. \quad (33)$$

From (30) and (32),

$$\begin{aligned} V_{\sigma(t_i)}(t_i) &\leq \mu_i V_{\sigma(t_{i-1})}(t_i) \\ &\leq \mu_i V_{\sigma(t_{i-1})}(t_{i-1})e^{-\lambda_{\sigma(t_{i-1})}T_i}. \end{aligned} \quad (34)$$

Iterating (34) for $i = 1$ to 4 yields

$$\begin{aligned} V_{\sigma(t_4)}(t_4) \leq \mu_4 V_{\sigma(t_3)}(t_4) \leq \\ \mu_4 V_{\sigma(t_3)}(t_3)e^{-\lambda_4 T_4} \leq \mu V_{\sigma(t_0)}(t_0)e^{-\lambda}, \end{aligned} \quad (35)$$

where μ, $\lambda \in \mathbb{R}$ are defined as

$$\mu \triangleq \mu_1\mu_2\mu_3\mu_4, \quad (36)$$
$$\lambda \triangleq \lambda_1 T_1 + \lambda_2 T_2 + \lambda_3 T_3 + \lambda_4 T_4. \quad (37)$$

Based on (27) and (35), the following inequality can be developed:

$$\begin{aligned} V_1(t_4) - V_1(t_0) &\leq -\left(1 - \mu e^{-\lambda}\right)V_1(t_0) \\ &\leq -\left(1 - \mu e^{-\lambda}\right)\gamma_{1_1}\|y(t_0)\|^2. \end{aligned} \quad (38)$$

This result can be generalized as

$$V_{\sigma(t_i)}(t_i + T) - V_{\sigma(t_i)}(t_i) \leq -\left(1 - \mu e^{-\lambda}\right)\gamma_{1_{\sigma(t_i)}}\|y(t_i)\|^2. \quad (39)$$

Provided α, k_s and β_p are selected sufficient large, and

$$1 - \mu e^{-\lambda} > 0, \quad (40)$$

(26), (27), (28), and (39) can be used to conclude asymptotic tracking [16, 17]. The switched control law $u(t) = u_{\sigma(t)}(t)$ ensures all closed-loop signals are bounded, and $|e(t)| \to 0$ as $t \to \infty$ in $\mathcal{D}$. The region of attraction $\mathcal{D}$ is defined as

$$\mathcal{D} \triangleq \mathcal{D}_1 \cap \mathcal{D}_2 \cap \mathcal{D}_3 \cap \mathcal{D}_4. \quad (41)$$

The region of attraction can be made arbitrarily large to include any initial conditions by increasing the control gain α and k_{s_p} (i.e., a semi-global type of stability result). □

6 Simulation study

Simulations are performed using the muscle model given in [19]. The controller computes a voltage as an input to the simulated muscle model. The simulation results are shown in Figs. 1−3. Desired trajectory is designed to simulate an average trajectory (cf. the experimental data in [15]) which is given as

$$q_d = 90 + pf + (ps - pf)(10(\frac{tt}{d})^3 - 15(\frac{tt}{d})^4 4 + 6(\frac{tt}{d})^5)), \quad (42)$$

where

$$T = 2.5s,$$
$$T_t = [0\ 0.12T\ 0.48T\ 0.62T\ T],$$
$$A = [0\ -7\ 10\ -20].$$

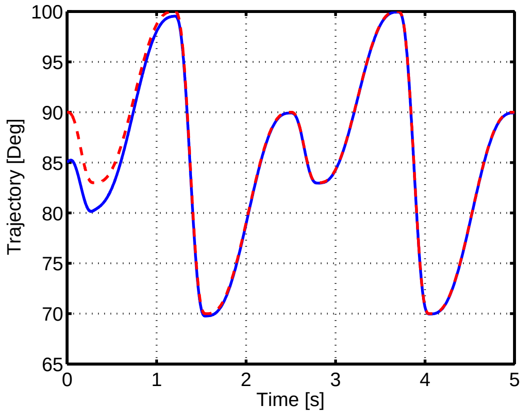

Figure 1. Actual (solid line) and desired (dashed line) trajectories.

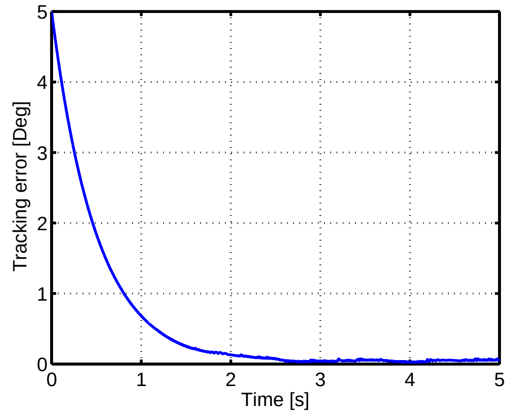

Figure 2. Tracking error.

$$
\begin{aligned}
pf &= A(i), \\
ps &= A(i+1), \\
tt &= t(\mathrm{mod}T) - T_t(i), \\
d &= T_t(i+1) - T_t(i), \\
i &= \begin{cases} 1 & 0 \le t(\mathrm{mod}T) < 0.12T \\ 2 & 0.12T \le t(\mathrm{mod}T) < 0.48T \\ 3 & 0.48T \le t(\mathrm{mod}T) < 0.62T \\ 4 & 0.62T \le t(\mathrm{mod}T) < T, \end{cases}
\end{aligned}
$$

where T is the gait period; T_t is the time period for each phase; A is the amplitude of each phase; and i is the phase indicator. The gains of the controller are selected as

$$
\begin{aligned}
\alpha &= 2, \\
k_s &= [5\ 5\ 5\ 5], \\
k_c &= [22\ 22\ 22\ 22], \\
\beta &= [0.2\ 1.2\ 0.4\ 0.3].
\end{aligned}
$$

The tracking performance is shown in Fig. 1. Asymptotic decrease of tracking error is depicted in Fig. 2 The control input is in the range of $19-25V$. The control input is within a typical range and the tracking error indicate the controller can yield functional gaits.

7 Conclusion

Precise and accurate ankle movement control has the potential to improve the capabilities of rehabilitation effects for people with certain neurological disorders. A switched sliding mode based controller is developed to ensure that the ankle tracks a designed or recorded trajectory during gait which can be used for gait retraining. Semi-global asymptotic tracking is obtained for the switched controller during gait, which is analyzed based on multiple Lyapunov functions and the performance is illustrated though simulations. Experimental testing is in progress.

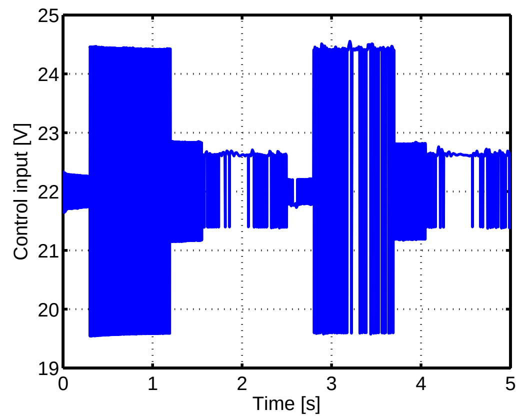

Figure 3. Computed voltage as control input.

REFERENCES

[1] Duncan, P. W., Sullivan, K. J., Behrman, A. L., Azen, S. P., Wu, S. S., Nadeau, S. E., Dobkin, B. H., Rose, D. K., Tilson, J. K., and Team, L. E. A. P. S. I., 2007. "Protocol for the locomotor experience applied post-stroke (LEAPS) trial: a randomized controlled trial.". *BMC Neurol,* **7**, p. 39.

[2] Embrey, D. G., Holtz, S. L., Alon, G., Brandsma, B. A., and McCoy, S. W., 2010. "Functional electrical stimulation to dorsiflexors and plantar flexors during gait to improve walking in adults with chronic hemiplegia.". *Arch. Phys. Med. Rehabil.,* **91**(5), May, pp. 687–696.

[3] Kesar, T. M., Perumal, R., Reisman, D. S., Jancosko, A., Rudolph, K. S., Higginson, J. S., and Binder-Macleod, S. A., 2009. "Functional electrical stimulation of ankle plantarflexor and dorsiflexor muscles: effects on poststroke gait.". *Stroke,* **40**(12), Dec, pp. 3821–3827.

[4] Abbas, J. J., and Chizeck, H. J., 1991. "Feedback control of coronal plane hip angle in paraplegic subjects using functional neuromuscular stimulation". *IEEE Trans. Biomed. Eng.,* **38**(7), pp. 687–698.

[5] Schauer, T., Negard, N. O., Previdi, F., Hunt, K. J., Fraser, M. H., Ferchland, E., and Raisch, J., 2005. "Online identification and nonlinear control of the electrically stimulated quadriceps muscle". *Control Eng. Pract.,* **13**, pp. 1207–1219.

[6] Stegath, K., Sharma, N., Gregory, C., and Dixon, W. E., 2007. "An extremum seeking method for non-isometric neuromuscular electrical stimulation". In Proc. IEEE Int. Conf. Syst. Man Cybern., pp. 2528–2532.

[7] Lan, N., Feng, H., and Crago, E., 1994. "Neural network generation of muscle stimulation patterns for control of arm movements". *IEEE Trans. Rehabil. Eng.,* **2**(4), pp. 213–224.

[8] Abbas, J. J., and Chizeck, H. J., 1995. "Neural network control of functional neuromuscular stimulation systems: computer simulation studies". *IEEE Trans. Biomed. Eng.,* **42**(11), Nov., pp. 1117–1127.

[9] Chang, G.-C., Lub, J.-J., Liao, G.-D., Lai, J.-S., Cheng, C.-K., Kuo, B.-L., and Kuo, T.-S., 1997. "A neuro-control system for the knee joint position control with quadriceps stimulation". *IEEE Trans. Rehabil. Eng.,* **5**(1), Mar., pp. 2–11.

[10] Giuffrida, J. P., and Crago, P. E., 2005. "Functional restoration of elbow extension after spinal-cord injury using a neural network-based synergistic FES controller". *IEEE Trans. Neural Syst. Rehabil. Eng.,* **13**(2), pp. 147–152.

[11] Pedrocchi, A., Ferrante, S., De Momi, E., and Ferrigno, G., 2006. "Error mapping controller: a closed loop neuroprosthesis controlled by artificial neural networks". *J. Neuroeng. Rehabil.,* **3**(1), p. 25.

[12] Ajoudani, A., and Erfanian, A., 2009. "A neuro-sliding-mode control with adaptive modeling of uncertainty for control of movement in paralyzed limbs using functional electrical stimulation". *IEEE Trans. Biomed. Eng.,* **56**(7), July, pp. 1771–1780.

[13] Sharma, N., Gregory, C. M., Johnson, M., and Dixon, W. E., 2008. "Modified neural network-based electrical stimulation for human limb tracking". In Proc. IEEE Int. Symp. Intell. Control, pp. 1320–1325.

[14] Sharma, N., Stegath, K., Gregory, C. M., and Dixon, W. E., 2009. "Nonlinear neuromuscular electrical stimulation tracking control of a human limb". *IEEE Trans. Neural Syst. Rehabil. Eng.,* **17**(6), pp. 576–584.

[15] Perry, J., 1992. *Gait analysis : normal and pathological function*. Harry C. Benson.

[16] Liberzon, D., and Morse, A., 1999. "Basic problems in stability and design of switched systems". *IEEE Contr. Syst. Mag.,* **19**(5), pp. 59–70.

[17] Goebel, R., Sanfelice, R., and Teel, A., 2009. "Hybrid dynamical systems". *IEEE Contr. Syst. Mag.,,* **29**(2), pp. 28 –93.

[18] Ferrarin, M., and Pedotti, A., 2000. "The relationship between electrical stimulus and joint torque: A dynamic model". *IEEE Trans. Rehabil. Eng.,* **8**(3), pp. 342–352.

[19] Ferrarin, M., Palazzo, F., Riener, R., and Quintern, J., 2001. "Model-based control of FES-induced single joint movements". *IEEE Trans. Neural Syst. Rehabil. Eng.,* **9**(3), Sept., pp. 245–257.